

# Influence of final state interaction on incoherent $\eta$ -photoproduction on the deuteron near threshold <sup>\*</sup>

A. Fix<sup>†</sup> and H. Arenhövel

*Institut für Kernphysik, Johannes Gutenberg-Universität, D-55099 Mainz, Germany*

(November 29, 2017)

## Abstract

Incoherent  $\eta$ -photoproduction on the deuteron is studied for photon energies from threshold up to 720 MeV. The elementary  $\gamma N \rightarrow \eta N$  amplitude is constructed in the frame of a conventional isobar model. Effects of final state interaction are investigated and their role in the cross section as well as in polarization observables is found to be important. Inclusion of such effects leads to a satisfactory agreement with experimental data in the near threshold region. In addition, recent experimental results on the coherent reaction  $d(\gamma, \eta)d$  are discussed.

PACS numbers: 13.60. Le, 21.45. +v, 25.20. Lj

Typeset using REVTeX

---

<sup>\*</sup>Supported by the Deutsche Forschungsgemeinschaft (SFB 201)

<sup>†</sup>Supported by the Deutscher Akademischer Austauschdienst

## I. INTRODUCTION

The main motivation for studying  $\eta$ -photoproduction on the deuteron is to obtain information on the elementary process on the neutron. The evident advantages of using a deuteron target are (i) the small binding energy of nucleons in the deuteron, which from the kinematical point of view provides the case of a nearly free neutron target, and (ii) minimal number of nucleons, reducing the influence of a nuclear environment on the elementary production process and allowing a careful microscopic treatment. The interest in the elementary process on the neutron is closely connected with the question concerning the isotopic structure of the  $S_{11}(1535)$  photoexcitation amplitude. A combined analysis of  $\gamma p \rightarrow \eta p$ ,  $\gamma d \rightarrow \eta d$  and inclusive  $\gamma d \rightarrow \eta X$  reactions [1,2] have confirmed its predominantly isovector character as predicted by quark models [3]. Furthermore, very recently exclusive measurements of the  $(\gamma, \eta N)$  reaction on the deuteron for quasifree kinematics with detection of forward emerging nucleons in coincidence with etas were performed [4]. This experiment, providing direct information on the ratio  $\sigma_n/\sigma_p$ , is expected to be quite precise, since the experimental systematic errors as well as different model corrections will largely cancel. From the data of [4] the ratio  $\alpha = t_{\gamma\eta}^{(s)}/t_{\gamma\eta}^{(p)}$  of the isoscalar to the proton amplitude is extracted as  $\alpha_{qf} = 0.09 \pm 0.02$ . At the same time, if one wants to find agreement between the data on the coherent  $\gamma d \rightarrow \eta d$  cross section of [4] and conventional impulse approximation calculations [5,6], one needs a considerably larger parameter  $\alpha_{coh} = 0.20 \pm 0.02$ . If one assumes that the value  $\alpha_{qf}$  is more reliable, one is lead to the conclusion that the impulse approximation fails in describing the coherent reaction. Thus one either would need to search for new mechanisms dominating the coherent process or one would need to question the accuracy of the experimental data.

It should be noted, that the method of extracting the information about the single nucleon processes from the deuteron data is based on the so-called spectator-nucleon model, in which the pure quasifree production is considered as the only mechanism for the knock-out  $d(\gamma, \eta N)N$  reaction. Therefore, a careful investigation of the validity of this approximation,

i.e., the estimation of possible other effects is needed. The main goal of the present work is to study the role of rescattering in the final state of the  $\gamma d \rightarrow \eta np$  process. One can expect that such effects become important close to the reaction threshold. In this region the smallness of the excitation energy in the final  $np$ -system and the large momentum transfer (which is about the  $\eta$  mass in the  $\gamma d$  c.m. frame) lead to a kinematical situation, where two final nucleons move primarily together with a large total, but small relative momentum. For this kinematics, the spectator model is expected to give a very small cross section since the momenta of both nucleons are large and, on the other hand, the corrections due to the strong  $NN$ -interaction may be significant. Furthermore, as has been shown in [7], the  $\eta$ -rescattering can also visibly change the  $\gamma d \rightarrow \eta np$  cross section near threshold.

In Section II we present the isobar model for the elementary  $\eta$ -photoproduction process. The treatment of the  $\gamma d \rightarrow \eta np$  amplitude, based on time-ordered perturbation theory including  $\eta N$  and  $NN$ -rescattering, is developed in Section III. A similar approach was adopted for the analysis of coherent  $\pi^0$ -photoproduction on the deuteron [8]. In our notation, we follow mainly this paper. In this Section, we also discuss the effects of rescattering on cross sections and polarization observables and compare our results with available experimental data. Finally, some attention is paid to the interpretation of experimental results of Ref. [4] on the coherent process.

## II. THE $\gamma N \rightarrow \eta N$ AMPLITUDE

As a starting point we consider the elementary process

$$\gamma(k_\mu, \vec{\varepsilon}_\lambda) + N(p_\mu) \rightarrow \eta(q_\mu) + N(p'_\mu), \quad (1)$$

which we need as input for studying the  $\eta$ -photoproduction on the deuteron. The four momenta of the participating particles are denoted by

$$k_\mu = (\omega, \vec{k}), \quad q_\mu = (\omega_{\vec{q}}, \vec{q}), \quad p_\mu = (E_{\vec{p}}, \vec{p}), \quad p'_\mu = (E_{\vec{p}'}, \vec{p}'), \quad (2)$$

and  $\vec{\varepsilon}_\lambda$  stands for the photon polarization vector. The particle energies are

$$\omega = k, \quad \omega_{\vec{q}} = \sqrt{q^2 + m_\eta^2}, \quad E_{\vec{p}'^{(v)}} = \sqrt{p'^{(v)2} + M_N^2}, \quad (3)$$

where  $M_N$  and  $m_\eta$  are the masses of nucleon and  $\eta$  meson, and  $k$ ,  $q$ ,  $p$ , and  $p'$  denote the absolute values of the respective three-momenta.

Past studies [9,10,11,12] of the  $p(\gamma, \eta)p$  process for photon lab energies from threshold up to 800 MeV have clearly shown the dominant role of the  $S_{11}(1535)$  resonance which decays with a relatively large probability into the  $\eta N$  channel. For this reason we have chosen a non-relativistic isobar model, in which the  $\eta$ -photoproduction proceeds exclusively through the electric dipole transition to the  $S_{11}(1535)$  (hereafter denoted by  $N^*$ ). Possible background contributions, such as nucleon pole and vector meson exchange, are neglected because of their insignificance in the energy region under consideration. Within the mentioned model the elementary  $\eta$ -photoproduction amplitude in an arbitrary frame of reference reads

$$t_{\gamma\eta}(W_{\gamma N}) = v_{\eta N^*}^\dagger g_{N^*}(W_{\gamma N}) v_{\gamma N^*}, \quad (4)$$

where  $W_{\gamma N}$  is the  $\gamma N$  invariant mass. The nonrelativistic current for the electromagnetic vertex  $v_{\gamma N^*} = -\vec{\epsilon}_\lambda \cdot \vec{j}_{N^*N}$  is given by

$$\vec{j}_{N^*N} = e \frac{k_{\gamma N}}{M_{N^*} + M_N} g_{\gamma NN^*} \vec{\sigma}, \quad (5)$$

where  $M_{N^*}$  is the resonance mass and  $k_{\gamma N}$  stands for the relative photon-nucleon momentum

$$\vec{k}_{\gamma N} = \frac{M_N \vec{k} - (M_{N^*} - M_N) \vec{p}}{M_{N^*}}. \quad (6)$$

The vertex constant  $g_{\gamma NN^*}$  can be expressed in terms of the helicity amplitude  $A_{1/2}^N$  of the  $N^*$  photoexcitation

$$e g_{\gamma NN^*} = \sqrt{\frac{2M_{N^*}(M_{N^*} + M_N)}{M_{N^*} - M_N}} A_{1/2}^N. \quad (7)$$

Furthermore, we introduce the isoscalar  $g_{\gamma NN^*}^{(s)}$  and isovector  $g_{\gamma NN^*}^{(v)}$  coupling constants in accordance with the isotopic structure of the photoproduction amplitude for an isoscalar meson

$$g_{\gamma NN^*} = g_{\gamma NN^*}^{(s)} + \tau_3 g_{\gamma NN^*}^{(v)}. \quad (8)$$

For the hadronic vertex  $v_{\eta N^*}^\dagger$  we use the pseudoscalar coupling

$$v_{\eta N^*}^\dagger = -i g_{\eta NN^*}. \quad (9)$$

Finally, the  $N^*$  propagator

$$g_{N^*}(W_{\gamma N}) = \frac{1}{W_{\gamma N} - M_{N^*} + \frac{i}{2}\Gamma(W_{\gamma N})} \quad (10)$$

involves the energy dependent decay width

$$\Gamma = \Gamma_{\eta N} + \Gamma_{\pi N} + \Gamma_{\pi\pi N}. \quad (11)$$

The partial  $\eta N$  and  $\pi N$  widths are related to the corresponding coupling constants in our nonrelativistic approach

$$\Gamma_{xN}(W_{\gamma N}) = \frac{g_{xNN^*}^2}{4\pi} \frac{2M_N}{W_{\gamma N}} q_x^*, \quad (x = \eta, \pi), \quad (12)$$

where  $q_x^*$  is the momentum of the respective particle in the  $\gamma N$  c.m. system. Following Ref. [5] we treat the  $N^*$  width for the  $\pi\pi N$  channel purely phenomenologically, as a constant above  $\pi\pi N$  threshold.

Thus the full  $\eta$ -photoproduction amplitude may be written in the form

$$t_{\gamma\eta}^{(s/v)} = e g_{\eta NN^*} \frac{k_{\gamma N}}{M_{N^*} + M_N} \frac{g_{\gamma NN^*}^{(s/v)}}{W_{\gamma N} - M_{N^*} + \frac{i}{2}\Gamma(W_{\gamma N})} i\vec{\sigma} \cdot \vec{\varepsilon}_\lambda. \quad (13)$$

In the actual calculation we use the following set of  $N^*$  parameters

$$M_{N^*} = 1535 \text{ MeV}, \quad g_{\eta NN^*} = 2.10, \quad g_{\pi NN^*} = 1.19, \quad \Gamma_{\pi\pi N} = 16 \text{ MeV}, \quad (14)$$

which gives for the total and partial decay widths at the resonance position  $W_{\gamma N} = M_{N^*}$

$$\Gamma = 160 \text{ MeV}, \quad \Gamma_{\eta N} = 0.5 \Gamma, \quad \Gamma_{\pi N} = 0.4 \Gamma, \quad \Gamma_{\pi\pi N} = 0.1 \Gamma. \quad (15)$$

This parametrization is reasonably consistent with the values following from the 1996 PDG listings [13]. The amplitude (13) gives quite a good description of the  $\gamma p \rightarrow \eta p$  total cross section data [9] (see Fig. 1) if we take for the proton helicity amplitude the value  $A_{1/2}^p = 104 \cdot 10^{-3} \text{ GeV}^{-1/2}$ .

### III. THE $\gamma D \rightarrow \eta NP$ REACTION

Now we turn to incoherent  $\eta$ -photoproduction on the deuteron

$$\gamma(k_\mu, \vec{\varepsilon}_\lambda) + d(Q_\mu) \rightarrow \eta(q_\mu) + N_1(p_{1\mu}) + N_2(p_{2\mu}). \quad (16)$$

The momenta of all particles are defined similarly to those in Section II. We restrict ourselves to the small region of incident photon energies from threshold up to 720 MeV. All calculations refer to the laboratory frame,  $Q_\mu = (M_d, \vec{0})$ , unless otherwise noted. The coordinate system is chosen to have a right-hand orientation with  $z$ -axis along the photon momentum  $\vec{k}$  and  $y$ -axis parallel to  $\vec{k} \times \vec{q}$ . We work in the isospin formalism and consider the two outgoing nucleons symmetrically, not specifying their isotopic states. The ratio  $\alpha = t_{\gamma\eta}^{(s)}/t_{\gamma\eta}^{(p)}$  is taken to be 0.11, which, as will be discussed below, produces the best agreement with experimental data. The laboratory cross section for the reaction (16) with unpolarized particles reads

$$d\sigma = \frac{1}{(2\pi)^5} \delta^4(k_\mu + Q_\mu - q_\mu - p_{1\mu} - p_{2\mu}) \frac{1}{6} \sum_{\lambda m_d} \sum_{S m_S T} |M_{S m_S T, \lambda m_d}|^2 \frac{M_N^2}{2\omega} \frac{d^3 q}{2\omega_{\vec{q}}} \frac{d^3 p_1}{E_{\vec{p}_1}} \frac{d^3 p_2}{E_{\vec{p}_2}}, \quad (17)$$

where  $M_{S m_S T, \lambda m_d}$  denotes the reaction amplitude

$$M_{S m_S T, \lambda m_d} = \langle \vec{q}, \vec{p}_1 \vec{p}_2, S m_S T | M_\lambda | m_d \rangle. \quad (18)$$

Here  $m_d$  stands for the deuteron spin projection, and the final two nucleon state is specified by the nucleon momenta  $\vec{p}_1, \vec{p}_2$  as well as by spin  $S m_S$  and isospin  $T(m_T = 0)$  quantum numbers. The corresponding fully antisymmetric  $NN$ -function can formally be written as

$$|\vec{p}_1 \vec{p}_2, S m_S T\rangle = \frac{1}{\sqrt{2}} \left( |\vec{p}_1 \vec{p}_2, S m_S\rangle - (-1)^{S+T} |\vec{p}_2 \vec{p}_1, S m_S\rangle \right). \quad (19)$$

The deuteron wave function in (18) is noncovariantly normalized to unity. The Fourier transform of its internal part separating the spin part has the familiar form

$$\begin{aligned} \phi_{m_S m_d}(\vec{p}) &= \langle \vec{p}, 1 m_S | 1 m_d \rangle \\ &= (2\pi)^{3/2} \sum_{L=0,2} \sum_{m_L} i^L u_L(p) (L m_L 1 m_S | 1 m_d) Y_{L m_L}(\hat{p}). \end{aligned} \quad (20)$$

For the radial functions  $u_L(p)$  we use the parametrization of the Bonn-potential model (OBEPQ-version) [14]. The main features of the process (16) will be investigated by considering the partially integrated cross sections  $d\sigma/dq d\Omega_{\vec{q}}$  and  $d\sigma/d\Omega_{\vec{q}}$ , which are obtained from the fully exclusive cross section

$$\frac{d\sigma}{d\Omega_{\vec{p}} dq d\Omega_{\vec{q}}} = (2\pi)^4 \mathbf{K} \frac{1}{6} \sum_{\lambda m_d} \sum_{S m_S T} |M_{S m_S T, \lambda m_d}|^2 \quad (21)$$

by appropriate integration. Here, the kinematic factor

$$\mathbf{K} = \frac{1}{(2\pi)^9} \frac{p^3 q^2 M_N^2}{4\omega\omega_{\vec{q}} \left| E_{\vec{p}_1} \left( p^2 + \frac{1}{2} \vec{P} \cdot \vec{p} \right) + E_{\vec{p}_2} \left( p^2 - \frac{1}{2} \vec{P} \cdot \vec{p} \right) \right|} \quad (22)$$

is expressed in terms of relative  $\vec{p} = (\vec{p}_2 - \vec{p}_1)/2$  and total  $\vec{P} = \vec{p}_1 + \vec{p}_2$  momenta of the two final nucleons. We prefer this choice of variables, because in this case the kinematic factor does not have any singularity on the boundary of the available phase space, when  $p \rightarrow 0$  [15]. With respect to polarization observables, we consider in this work only the tensor asymmetries  $T_{2M}$  of the deuteron target, which, as will be discussed, is most sensitive to the effects of rescattering. For this observable, we use the definition similar to that given in Ref. [16] for deuteron photodisintegration

$$T_{2M} \frac{d\sigma}{dq d\Omega_{\vec{q}}} = (2 - \delta_{M0}) \Re \epsilon V_{2M}, \quad M = 0, 1, 2, \quad (23)$$

where

$$V_{2M} = \sqrt{\frac{5}{3}} \sum_{m'_d m_d} \sum_{S m_S T \lambda} (-1)^{1-m'_d} \begin{pmatrix} 1 & 1 & 2 \\ m_d & -m'_d & -M \end{pmatrix} \int \mathbf{K} M_{S m_S T, \lambda m_d}^* M_{S m_S T, \lambda m'_d} d\Omega_{\vec{p}}. \quad (24)$$

Thus, for example, the asymmetry  $T_{20}$  is given by the expression

$$T_{20} = \frac{1}{\sqrt{2}} \frac{\sum_{S m_S T \lambda} \int \mathbf{K} \left( |M_{S m_S T, \lambda 1}|^2 + |M_{S m_S T, \lambda -1}|^2 - 2|M_{S m_S T, \lambda 0}|^2 \right) d\Omega_{\vec{p}}}{\sum_{\lambda m_d} \sum_{S m_S T} \int \mathbf{K} |M_{S m_S T, \lambda m_d}|^2 d\Omega_{\vec{p}}}. \quad (25)$$

Then, the cross section can be expressed in terms of the unpolarized cross section and the tensor target asymmetry as

$$\frac{d\sigma(P_2^d)}{dq d\Omega_{\vec{q}}} = \frac{d\sigma}{dq d\Omega_{\vec{q}}} \left[ 1 + P_2^d \sum_{M \geq 0} T_{2M} \cos(M\phi_d) d_{M0}^2(\theta_d) \right], \quad (26)$$

where  $P_d^2$  is the degree of deuteron tensor polarization with respect to the orientation for which the deuteron density matrix is diagonal and which is characterized by the angles  $\theta_d$  and  $\phi_d$  in the chosen coordinate system.

The transition matrix elements  $M_{Sm_S T, \lambda m_d}$  are calculated in the frame of time-ordered perturbation theory, using the electromagnetic and hadronic vertices, introduced in Section II. As full amplitude we include besides the pure impulse approximation (IA) one-loop  $NN$ - and  $\eta N$ -rescattering terms as shown in Fig. 2

$$M_{Sm_S T, \lambda m_d} = M_{Sm_S T, \lambda m_d}^{IA} + M_{Sm_S T, \lambda m_d}^{NN} + M_{Sm_S T, \lambda m_d}^{\eta N}. \quad (27)$$

Another possible two-step  $\eta$ -production mechanism in the two-nucleon system  $\gamma N \rightarrow \pi N \rightarrow \eta N$  gives a negligible contribution as was shown in [7]. We now will consider successively all three terms and investigate their role in the reaction (16).

### A. The impulse approximation (IA)

The matrix element given by the diagramm (a) in Fig. 2 reads

$$M_{Sm_S T, \lambda m_d}^{IA} = -\langle \vec{q}, \vec{p}_1 \vec{p}_2, Sm_S T | V_{\eta N^*}^\dagger G_{N^* N}(W_{\gamma N}) \vec{\varepsilon}_\lambda \cdot \vec{J}_{N^* N} | m_d \rangle. \quad (28)$$

The effective one-particle operators for the hadronic vertex  $V_{\eta N^*}^\dagger$  and current  $\vec{J}_{N^* N}$  are defined using (5) through (9) as

$$V_{\eta N^*}^\dagger = v_{\eta N^*}^\dagger(1) + v_{\eta N^*}^\dagger(2), \quad (29)$$

$$\vec{J}_{N^* N} = \vec{j}_{N^* N}(1) + \vec{j}_{N^* N}(2), \quad (30)$$

with arguments, referring to nucleon 1 and 2. The propagator for the  $N^* N$  intermediate state is

$$G_{N^* N}(W_{\gamma N}) = \frac{1}{W_{\gamma N} - M_{N^*} + \frac{i}{2}\Gamma(W_{\gamma N})}, \quad (31)$$

with  $W_{\gamma N}$  being the energy available for the  $N^*$  excitation



$$W_{\gamma N} = \omega + M_d - M_N - \frac{p_N^2}{2M_N} - \frac{p_{N^*}^2}{2M_{N^*}}. \quad (32)$$

In the deuteron lab system we have  $\vec{p}_{N^*} = \vec{k} - \vec{p}_N$ . Taking plane waves for all three outgoing particles, the expression (28) can be reduced to the form

$$M_{S m_S T, \lambda m_d}^{IA} = \sum_{m'_S} \langle S m_S | \left[ t_{\gamma\eta}^{(T)}(W_{\gamma N_1}) \phi_{m'_S m_d}(\vec{p}_2) - (-1)^{S+T} t_{\gamma\eta}^{(T)}(W_{\gamma N_2}) \phi_{m'_S m_d}(\vec{p}_1) \right] | m_d \rangle, \quad (33)$$

with upper index ( $T$ ) referring to the isoscalar ( $s$ ) or the isovector ( $v$ ) amplitude (13) for  $T = 0$  and  $T = 1$ , respectively. The energy  $W_{\gamma N_i}$  is defined in (32) with  $\vec{p}_N = \vec{p}_{2(1)}$  for  $i=1(2)$ . The amplitude (33) corresponds to the simple spectator-nucleon model. The elementary operator  $t_{\gamma\eta}^{(s/v)}$  produces the  $(\gamma, \eta)$  process on the nucleon, which takes the whole photon energy available after meson production. Since in our approach the spectator nucleon is taken to be on-shell, the active nucleon is off-shell as determined by the energy and momentum conservation at the corresponding vertex

$$\vec{p} = \vec{q} + \vec{p}_i - \vec{k}, \quad (34)$$

$$E_{\vec{p}} = \omega_{\vec{q}} + E_{\vec{p}_i} - \omega \quad (i = 1, 2). \quad (35)$$

In order to qualitatively explain the approximations concerning the rescattering terms, discussed below, we would like to demonstrate here some features of the reaction amplitude keeping in (27) only the impulse approximation. Due to the large transferred momentum associated with the large  $\eta$  mass, the  $\eta$ -angular distribution shows a fast decrease with increasing angle, so that the major part of the cross section is concentrated in the forward direction. Therefore, we choose for the discussion the forward angle region. The differential cross section  $d\sigma/d\Omega_{\vec{q}}$  calculated within the spectator model is shown in Fig. 3 as a function of the lab photon energy, where in addition the separate contribution from the various important partial waves in the initial and final states are shown. Several conclusions can be drawn:

(i) Because of the large velocity of both outgoing nucleons near threshold, the high momentum components of the deuteron wave function become significant. As a consequence,

a few MeV above threshold a rather large contribution from the deuteron  $D$ -wave arises leading to a strong destructive interference between  ${}^3D_1$  and  ${}^3S_1$  states which reduces sizeably the pure  $S$ -wave cross section. With increasing photon energy, the role of the  $D$ -wave decreases rapidly, e.g., at  $\omega = 650$  MeV this reduction amounts to only 8%.

(ii) The separate contributions from the  ${}^1S_0$  and  ${}^3S_1$  states of the final  $NN$ -system clearly show the dominance of the singlet over the triplet  $s$ -wave. The strong suppression of the  ${}^3S_1$  state is due to the small isoscalar part of the  $\eta$ -photoproduction amplitude (in our calculation  $t_{\gamma\eta}^{(s)} \approx 0.12 t_{\gamma\eta}^{(v)}$ ) so that the transition from the deuteron bound state ( $T = 0, S = 1$ ) to the continuum  $NN$ -state ( $T = 1, S = 0$ ) is most probable. If one neglects the  $D$ -wave of the deuteron, the following approximate relation holds

$$\frac{d\sigma({}^1S_0)}{d\sigma({}^3S_1)} = \left| \frac{t_{\gamma\eta}^{(v)}}{t_{\gamma\eta}^{(s)}} \right|^2 \frac{\sum_{m_d} |\langle S=0 | \vec{\sigma} \cdot \vec{\epsilon} | m_d \rangle|^2}{\sum_{m_d} |\langle S=1 | \vec{\sigma} \cdot \vec{\epsilon} | m_d \rangle|^2} = \frac{1}{2} \left| \frac{t_{\gamma\eta}^{(v)}}{t_{\gamma\eta}^{(s)}} \right|^2 \approx 33. \quad (36)$$

This strong dominance of the singlet  $s$ -wave state is slightly reduced by the presence of the  $D$ -component, in particular near threshold.

## B. The $NN$ -rescattering

The diagram (b) in Fig. 2 describes the  $NN$ -rescattering whose amplitude is given by

$$M_{Sm_S T, \lambda m_d}^{NN} = -\langle \vec{q}, \vec{p}_1 \vec{p}_2, S m_S T | T_{NN} G_{NN} V_{\eta N^*}^\dagger G_{N^* N} (W_{\gamma N}) \vec{\epsilon}_\lambda \cdot \vec{J}_{N^* N} | m_d \rangle. \quad (37)$$

The free nonrelativistic propagator of the two nucleons in terms of the relative  $NN$ -momenta  $\vec{p} = (\vec{p}_2 - \vec{p}_1)/2$  and  $\vec{p}' = (\vec{p}'_2 - \vec{p}'_1)/2$  has the form

$$\langle \vec{p} | G_{NN} | \vec{p}' \rangle = \frac{M_N}{p^2 - p'^2 + i\epsilon}. \quad (38)$$

The  $NN$  dynamics in the final state is determined by the half-off-shell nucleon-nucleon  $t$ -matrix  $T_{NN}$ , which we evaluate for the same OBEPQ Bonn potential [14] as for the deuteron wave function. We restrict the  $NN$ -rescattering to the  ${}^1S_0$  state. This approximation is justified by the previous observation that due to the spin-isospin selection rules the contribution from the triplet  ${}^3S_1$  state is at least one order of magnitude smaller than

that from the  $^1S_0$  state. As for the higher partial waves, their distortion is expected to be of minor importance compared to the resonant  $^1S_0$ -wave, since in the kinematical region considered in this work the relative kinetic energy in the  $NN$ -system is less than 72 MeV (see also [17]). Within this approximation, a straightforward calculation yields finally

$$M_{001,\lambda m_d}^{NN} = M_N \sum_{m'_S} \langle 00 | \int \frac{2t_{\gamma\eta}^{(v)}(W_{\gamma N}) T_{NN}(p', p)}{p^2 - p'^2 + i\epsilon} \phi_{m'_S m_d}(\vec{p}_N) \frac{d^3 p'}{(2\pi)^3} | m_d \rangle, \quad (39)$$

with  $\vec{p}_N = \frac{\vec{k}-\vec{q}}{2} + \vec{p}'$ . Since, as was noticed above, the deuteron  $D$ -wave component plays a non-negligible role in the IA, it was also taken into account in the matrix element (39). The influence of  $NN$ -rescattering is demonstrated in Fig. 4 for the  $\eta$ -momentum distribution at a given angle  $\theta_\eta$ . As expected, the strong interaction between the final nucleons in the  $^1S_0$  state changes drastically the cross section for large  $\eta$  momentum values. When  $q$  reaches its maximum, the excitation energy  $E_{np}$  in the  $np$ -pair vanishes, and thus the resonant  $^1S_0$  state appears as a rather narrow peak. The same effect is noted for charged  $\pi$ -photoproduction on the deuteron [17] as well as for deuteron electrodisintegration [18]. In principle, the experimental observation of this peak in the high  $\eta$ -momentum spectrum may serve as another evidence for the isovector nature of the  $N^*$  photoexcitation. In the hypothetical case  $t_{\gamma\eta}^{(s)} \gg t_{\gamma\eta}^{(v)}$ , the low-energy  $NN$ -rescattering would be dominated by the  $^3S_1$  state, which does not exhibit any resonant behaviour at  $E_{np} \approx 0$ .

In conclusion, one sees that the role of  $NN$ -rescattering is quite important, especially for small photon energies. At higher energies, the main part of the cross section is dominated by the IA, which gives a rather broad quasifree bump, where the role of  $NN$ -rescattering is expected to be of minor importance. The contribution from the deuteron  $D$ -wave is only significant close to threshold. Its effect is a destructive interference between the  $^3D_1 \rightarrow ^1S_0$  and the dominant  $^3S_1 \rightarrow ^1S_0$  transitions (see Fig. 4).

In Fig. 5 we depict also the tensor target asymmetries for  $\vec{d}(\gamma, \eta)np$  at two different photon energies. One readily notes that the asymmetry  $T_{20}$  is strongly affected by  $NN$ -rescattering. The reason for this is that  $T_{20}$  is directly defined by the difference between the cross section on the deuteron with spin parallel and perpendicular to the photon beam

direction (see (25)). Because of the spin-transverse form of the elementary operator (13), the transition  ${}^3S_1 \rightarrow {}^1S_0$  may occur in the  $\eta$ -photoproduction process with only opposite directions of photon and deuteron spin. Consequently, the strong  ${}^1S_0$  interaction between the final nucleons, enhancing the probability of this transition, increases the contribution from the matrix elements  $M_{Sm_S T, \lambda m_d}$  in (25) with  $m_d = \pm 1$ . The other target asymmetries,  $T_{22}$  and  $T_{11}$  which are not shown here, appear not to be sensitive to the  $NN$ -rescattering contribution. For the photon asymmetry  $\Sigma$  we have a trivial relation  $\Sigma = 0$ , which follows from our neglect of other terms besides the  $N^*$ -excitation amplitude in the elementary operator.

### C. The $\eta N$ -rescattering

The  $\eta N$ -rescattering amplitude given by the the diagram (c) in Fig. 2 reads

$$M_{Sm_S T, \lambda m_d}^{\eta N} = -\langle \vec{q}, \vec{p}_1 \vec{p}_2, Sm_S T | \frac{M_N}{2\mu W_{\eta N}} t_{\eta N} G_{\eta N} V_{\eta N^*}^\dagger G_{N^* N}(W_{\gamma N}) \vec{\epsilon}_\lambda \cdot \vec{J}_{N^* N} | m_d \rangle, \quad (40)$$

where  $\mu = \frac{M_N m_\eta}{M_N + m_\eta}$ . Similarly to the  $NN$ -case (38), we use the nonrelativistic propagator for the relative  $\eta N$ -motion

$$\langle \vec{q}_{\eta N} | G_{\eta N} | \vec{q}'_{\eta N} \rangle = \frac{2\mu}{q_{\eta N}^2 - q'_{\eta N}{}^2 + i\epsilon}. \quad (41)$$

In the spirit of our isobar approach, we consider the  $\eta N$ -interaction to proceed only via the  $N^*$  formation, which gives the  $t$ -matrix in the form

$$t_{\eta N}(W_{\eta N}) = v_{N^*}^\dagger g_{N^*}(W_{\eta N}) v_{N^*} = \frac{g_{\eta N N^*}^2}{W_{\eta N} - M_{N^*} + \frac{i}{2}\Gamma(W_{\eta N})}, \quad (42)$$

where  $W_{\eta N}$  is the  $\eta N$  invariant mass and other parameters are defined in Section II. Collecting the various pieces, we obtain for the amplitude (40)

$$M_{Sm_S T, \lambda m_d}^{\eta N} = \sum_{m'_S} \langle Sm_S | \int \left[ \frac{M_N}{W_{\eta N_2}} \frac{t_{\gamma\eta}^{(T)}(W_{\gamma N_1}) t_{\eta N}(W_{\eta N_2})}{q_{\eta N_2}^2 - q'_{\eta N}{}^2 + i\epsilon} \phi_{m'_S m_d}(\vec{p}_{N_2}) \right. \\ \left. - (-1)^{S+T} \frac{M_N}{W_{\eta N_1}} \frac{t_{\gamma\eta}^{(T)}(W_{\gamma N_2}) t_{\eta N}(W_{\eta N_1})}{q_{\eta N_1}^2 - q'_{\eta N}{}^2 + i\epsilon} \phi_{m'_S m_d}(\vec{p}_{N_1}) \right] \frac{d^3 q'_{\eta N}}{(2\pi)^3} | m_d \rangle, \quad (43)$$

with  $\vec{p}_{N_i} = \frac{\mu}{m_\eta}(\vec{k} - \vec{p}_i) + \vec{q}'_{\eta N}$  and  $\vec{q}_{\eta N_i} = \frac{m_\eta \vec{p}_i - M_N \vec{q}}{M_N + m_\eta}$  ( $i = 1, 2$ ).

The effect of  $\eta N$ -rescattering is demonstrated in Fig. 6 for the  $\eta$ -angular distribution in the  $\gamma d$  c.m. frame, where we also compare our results with experimental data for the inclusive reaction  $\gamma d \rightarrow \eta X$  [1]. In view of the small isoscalar part  $t_{\gamma\eta}^{(s)}$  of the elementary amplitude and the large momentum mismatch, the contribution from the coherent  $\gamma d \rightarrow \eta d$  process is expected to be negligible and, thus, the inclusive  $\eta$ -spectrum is dominated by the deuteron break-up channel. In the backward direction, the increase from  $\eta N$ -rescattering is in part kinematically enhanced. At these angles, the nucleons leave the interaction region with large momenta. Therefore, the spectator model gives a very small cross section underestimating the data by roughly a factor of 3 for  $\omega = 720$  MeV. In this situation, the  $\eta N$ -rescattering mechanism, allowing the large transferred momentum to be shared between two participating nucleons, becomes much more effective. The resonant character of the  $\eta N$ -interaction appears more pronounced at forward angles. Although its strong inelasticity decreases the cross section at high photon energies, close to threshold this effect is more than compensated by the attraction in the  $\eta N$ -system.

Finally, we show in Fig. 7 the total  $\gamma d \rightarrow \eta np$  cross section. One readily notes, that the simple spectator approach cannot describe the experimental data close to the threshold (see also [12]). As has been discussed in the Introduction, at small photon energies the spectator model considers the  $\gamma d \rightarrow \eta np$  process to proceed mainly through the high deuteron Fourier component, which appears only with small probability. The final state interaction provides a mechanism for bypassing this suppression. Our model predicts quite a significant contribution from  $NN$ -rescattering. It turns out to be dominant in the vicinity of the threshold and still increases the spectator results by about 10% at  $\omega = 720$  MeV. The  $\eta N$ -interaction is relatively less important, but is also significant mainly through the constructive interference between  $NN$ - and  $\eta N$ -rescattering contributions. With inclusion of the rescattering effects, we are able to reproduce the experimental cross section with  $\alpha = 0.11$ .

At this point, we would like to discuss briefly the possibility of extracting the ratio

$|t_{\gamma\eta}^{(n)}/t_{\gamma\eta}^{(p)}|$  from the corresponding ratio of exclusive  $d(\gamma, \eta n)p$  and  $d(\gamma, \eta p)n$  yields as has been done in Ref. [4]. Strictly speaking, the simple relation

$$\left| \frac{t_{\gamma\eta}^{(n)}}{t_{\gamma\eta}^{(p)}} \right| = \sqrt{\frac{d\sigma_{d(\gamma, \eta n)p}}{d\sigma_{d(\gamma, \eta p)n}}}, \quad (44)$$

consistent with a pure spectator approach is not valid away from quasifree kinematics, in particular, when final state interaction is taken into account. This is due to the fact, that rescattering “mixes” the single proton and neutron  $\eta$ -photoproduction processes, as is illustrated schematically in Fig. 8, taking as an example the  $NN$ -interaction term. Thus, in the region where the rescattering effects are dominant, the right hand side of (44) approximates unity in contrast to the elementary ratio.

In general, we can conclude from the above investigations, that the relation (44) works well for photon energies not too close to the threshold. As a confirmation, we have plotted in Fig. 9 the theoretical ratio  $\frac{d\sigma}{d\Omega_n}/\frac{d\sigma}{d\Omega_p}$  of the differential cross sections for the reaction  $d(\gamma, \eta N)N$  without and with rescattering versus the photon lab energy  $\omega$  and compare it to the corresponding value for free nucleons. The difference between the ratio for free nucleons and that for the deuteron, obtained within the spectator model, is due to the fact, that to the integration over nucleon momenta not only fast moving active nucleons but also slow ones partly contribute. One can see, that the additional final state interaction increases even more the ratio when approaching the threshold. However, for the energies considered in [4], its role is negligible, and from this point of view the validity of (44) is fully justified. The ratio of the neutron to the proton cross sections  $\sigma_n/\sigma_p = 0.61$ , corresponding to  $\alpha = 0.11$ , which we have used in this work and which reproduces well the  $\gamma d \rightarrow \eta X$  data of [1], slightly underestimates the one presented in Ref. [4]  $\sigma_n/\sigma_p = 0.68 \pm 0.06$ .

Finally, we would like to make a short comment on the coherent photoproduction process on the deuteron. We first note, that the sensitivity of the break-up cross section to a variation of  $\alpha$  is much less pronounced than for the coherent reaction, which is proportional to  $|t_{\gamma\eta}^{(s)}|^2$ . The present study within the isobar model has shown, that the experimental uncertainty in the  $\gamma d \rightarrow \eta np$  total cross section for photon energies between threshold and 720 MeV [1]

fixes the parameter  $\alpha$  within the limits of  $\alpha = 0.11 \pm 0.02$ . In Fig. 10 we demonstrate the strong sensitivity on  $\alpha$  of the  $\eta$ -angular distribution of the coherent reaction, which we have calculated within the conventional impulse approximation. In addition to the  $S_{11}(1535)$  resonance, the contributions from  $D_{13}(1520)$  as well as the nucleon pole term and  $\omega$ -meson exchange in the t-channel were included in the elementary operator (for further details see [20]). We do not touch here upon the question about the role of meson rescattering in the coherent reaction, which was investigated in [6,21,22]. However, one can expect, that due to its two-particle character, this effect will not strongly affect the coherent process in the region of forward  $\eta$ -angles which is associated with relatively small momentum transfer. As can be seen from Fig. 10 even the largest permissible value  $\alpha = 0.13$  gives a cross section, which is by more than a factor three below the data. Only with a rather large isoscalar amplitude corresponding to  $\alpha = 0.26$  the impulse approximation could describe the data well. This seeming inconsistency between the coherent and incoherent reaction with respect to the precise value of the parameter  $\alpha$  certainly needs further experimental and theoretical studies.

#### IV. CONCLUSION

We have studied incoherent  $\eta$ -photoproduction on the deuteron in the near threshold region. The elementary photoproduction amplitude, based on a pure isobar model, for which the  $\gamma NN^*$  and  $\eta NN^*$  vertices have been fitted, gives a good description of the experimental  $p(\gamma, \eta)p$  cross section data. As for the deuteron amplitude, we have considered in addition to the spectator-nucleon approach also  $NN$ -rescattering in the most important  $^1S_0$  channel and  $\eta N$ -rescattering. While the pure spectator model produces only a small fraction of the observed cross section near threshold, the strong attractive  $NN$ -interaction in the resonant  $^1S_0$  state enhances it considerably. The role of  $\eta N$ -rescattering is found to be less important. With inclusion of both rescattering effects we obtain quite a satisfactory agreement with the available data on the  $\gamma d \rightarrow \eta X$  differential and total cross sections, using as input for the

ratio of isoscalar to proton amplitude  $\alpha = 0.11$ . This value is roughly consistent with  $\alpha = 0.09 \pm 0.02$ , extracted from the recently measured ratio  $d\sigma_{d(\gamma,\eta p)}/d\sigma_{d(\gamma,\eta p)n}$ . Furthermore, we have shown, that this extraction can be justified within the frame of the pure spectator-nucleon model, since the role of final state interaction under the corresponding kinematical conditions is negligible.

### ACKNOWLEDGMENTS

A. F. is grateful to B. Krusche, R. Schmidt, M. Schwamb and P. Wilhelm for fruitful discussions. He would also like to thank the theory group of Professor H. Arenhövel as well as Professor H. Ströher, Monika Baumbusch and many scientists of the Institut für Kernphysik at the Mainz University for the very kind hospitality.



## REFERENCES

- [1] B. Krusche et al., Phys. Lett. **B358** (1995) 40
- [2] C. Bacci et al., Phys. Lett. **B28** (1969) 687
- [3] R. Koniuk, N. Isgur, Phys. Rev. **D21** (1980) 1868
- [4] P. Hoffmann-Rothe et al., submitted to Phys. Rev. Lett.
- [5] E. Breitmoser, H. Arenhövel, Nucl. Phys. **A612** (1997) 321
- [6] S. Kamalov, L. Tiator, C. Bennhold, Phys. Rev. **C55** (1997) 98
- [7] A.I. Fix, V.A. Tryasuchev, Yad. Fiz. **60** (1997) 41 (Phys. Atom. Nucl. **60** (1997) 35)
- [8] P. Wilhelm, H. Arenhövel, Nucl. Phys. **A593** (1995) 435; Nucl. Phys. **A609** (1996) 469
- [9] B. Krusche et al., Phys. Rev. Lett. **74** (1995) 3736
- [10] M. Benmerrouche, N.C. Mukhopadhyay, J.F. Zhang, Phys. Rev. **D51** (1995) 3237
- [11] L. Tiator, C. Bennhold, S.S. Kamalov, Nucl. Phys. **A580** (1994) 455
- [12] Ch. Sauermann, B.L. Friman, W. Nörenberg, Phys. Lett. **B341** (1995) 261
- [13] Review of Particle Properties, Phys. Rev. **D54** (1996) 1
- [14] R. Machleidt, K. Holinde, C. Elster, Phys. Rep. **149** (1987) 1
- [15] R. Schmidt, Diploma Thesis, Universität Mainz (1995)
- [16] H. Arenhövel, Few-Body Syst. **4** (1988) 55
- [17] J.-M. Laget, Nucl. Phys. **A296** (1978) 388
- [18] G.G. Simon, F. Borkowski, Ch. Schmitt, V.H. Walter, H. Arenhövel, W. Fabian, Phys. Rev. Lett. **37** (1976) 739 ; Nucl. Phys. **A324** (1979) 277
- [19] C. Sauermann, B.L. Friman, W. Nörenberg, GSI-Preprint-97-03; nucl-th/9701022

[20] A. Fix, H. Arenhövel, Mainz-Preprint-97-04; nucl-th/9703002 (Nucl. Phys. A in print)

[21] N. Hoshi, H. Hyuga, K. Kubodera, Nucl. Phys. A**324** (1979) 234

[22] D. Halderson, A.S. Rosenthal, Nucl. Phys. A**501** (1989) 856

FIGURES

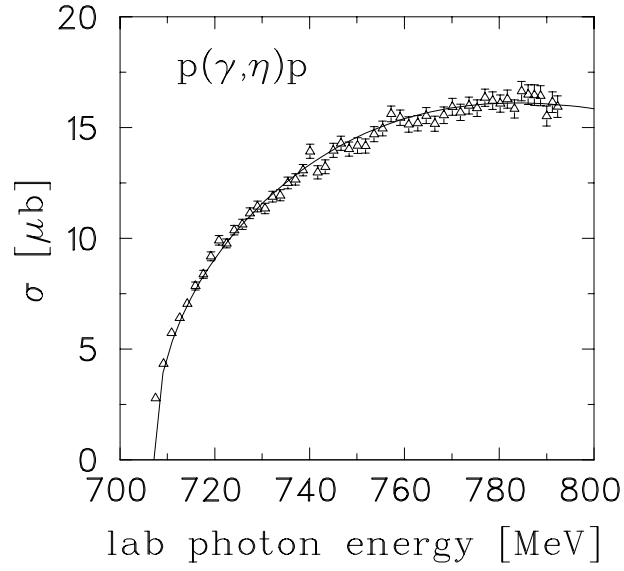


FIG. 1. The total cross section of the  $p(\gamma, \eta)p$  reaction. The experimental points are from Ref. [1].

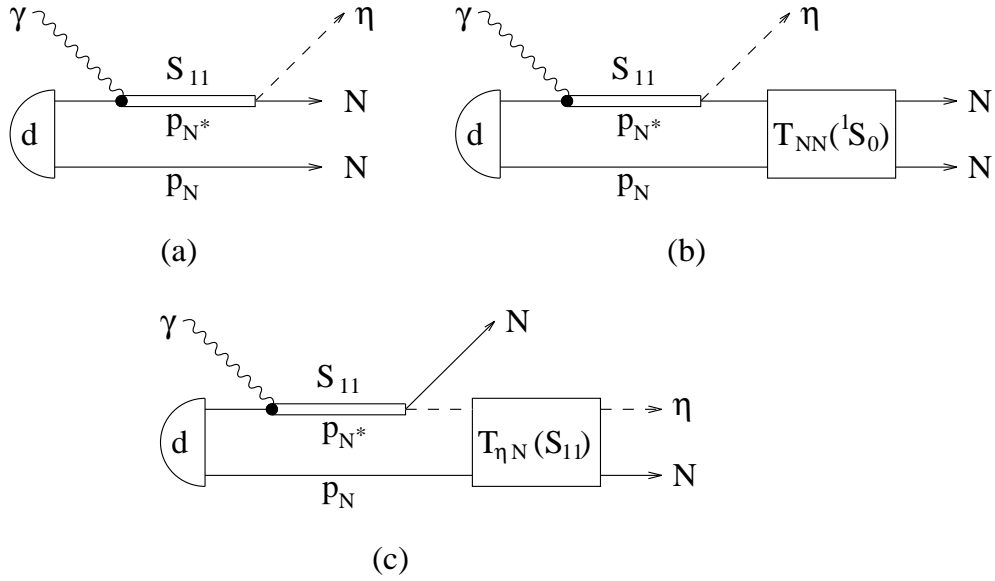


FIG. 2. Diagrammatic representation of the  $\gamma d \rightarrow \eta np$  amplitude, as studied in the present work: (a) impulse approximation, (b)  $NN$ -rescattering and (c)  $\eta N$ -rescattering.

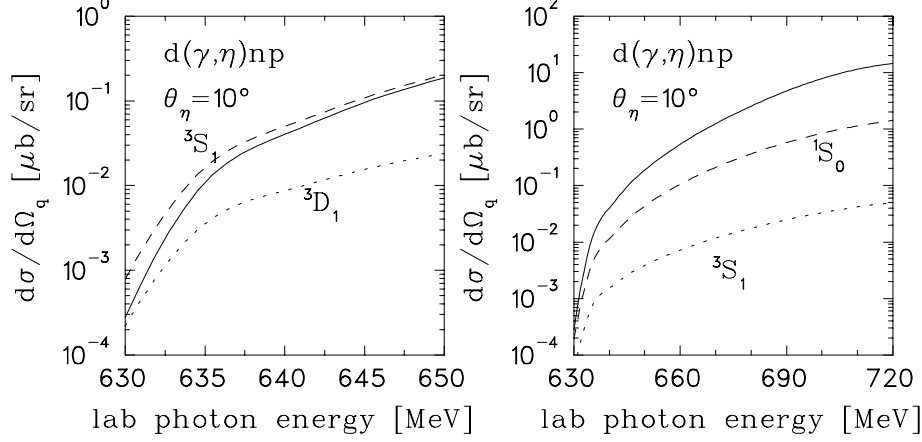


FIG. 3. The  $\eta$ -angular distribution in the  $\gamma d \rightarrow \eta np$  reaction, predicted by the IA (full curve). The contribution from the deuteron  ${}^3S_1$  and  ${}^3D_1$  components are separately shown in the left-hand panel. The right-hand panel presents the separate contributions from the final singlet  ${}^1S_0$  and triplet  ${}^3S_1$  waves.

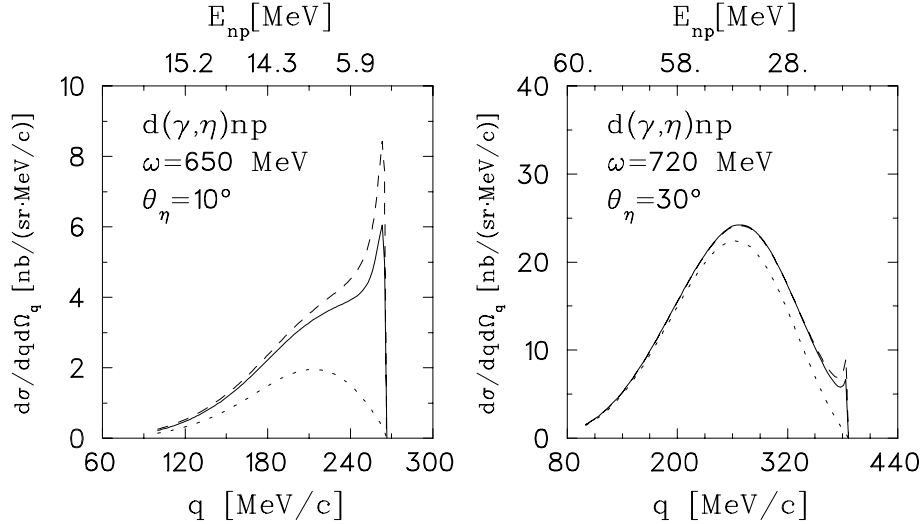


FIG. 4. The  $\eta$ -meson spectra at forward emission angles in the  $d(\gamma, \eta)np$  reaction for two different photon energies and angles. The dotted curves show the pure impulse approximation, whereas the full curves include the interaction between the outgoing nucleons. The dashed curves represent the results obtained without the  $D$ -wave contribution to the  $NN$ -rescattering amplitude. The excitation energy  $E_{np}$  in the final  $NN$ -system is indicated at the top abscissa.

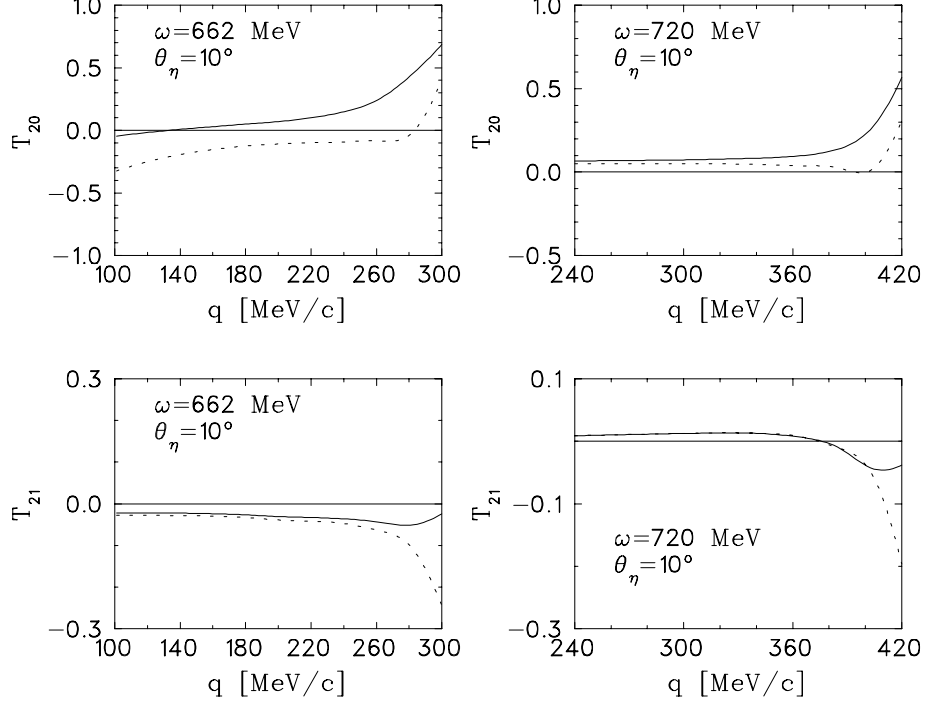


FIG. 5. Influence of  $NN$ -rescattering on several tensor target asymmetries for two photon lab energies as function of the  $\eta$ -momentum. Notation of the curves as in Fig. 4.

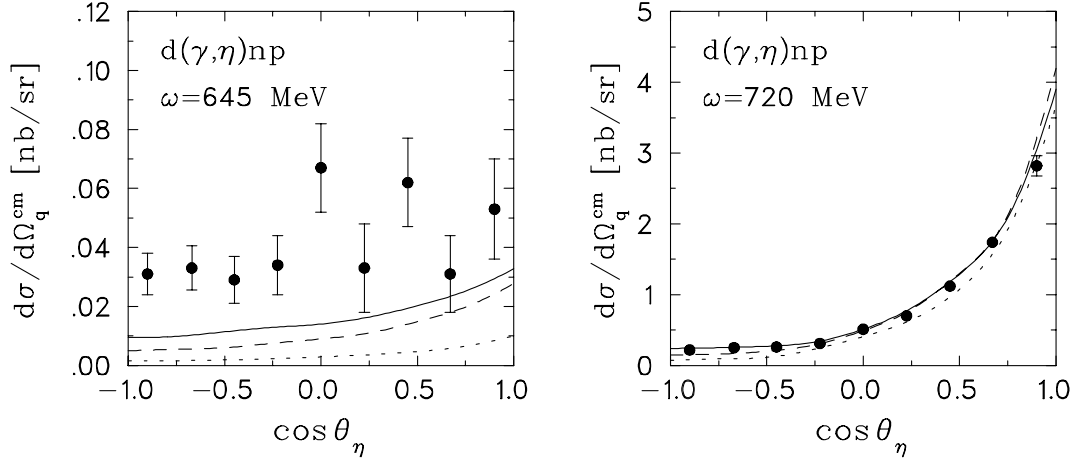


FIG. 6. The differential  $d(\gamma, \eta)np$  cross section, calculated in the  $\gamma d$  c.m. frame. Shown are the IA prediction (dotted lines), the successive addition of  $NN$  (dashed lines) and  $\eta N$  (full lines) rescattering. The experimental points represent the inclusive  $\gamma d \rightarrow \eta X$  measurements from Ref. [1].

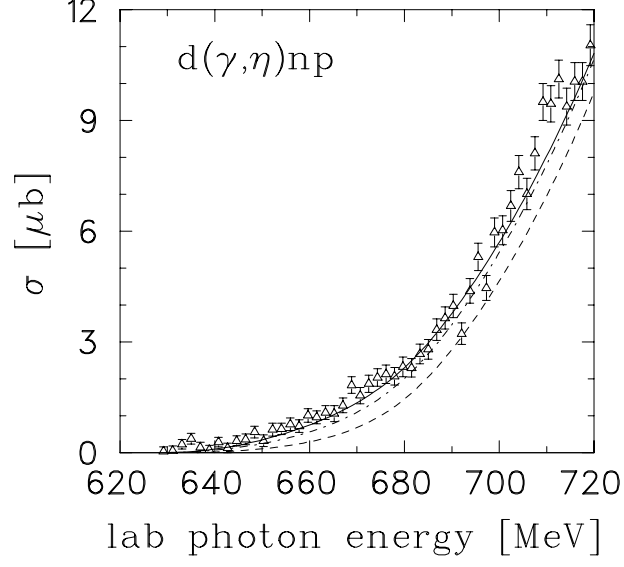


FIG. 7. Results of our calculations for the total  $\gamma d \rightarrow \eta np$  cross section compared with inclusive  $\gamma d \rightarrow \eta X$  experimental data [1]. The full and dashed lines represent the results obtained with and without allowance for rescattering of the final particles, respectively. The dash-dotted line includes only IA and  $NN$ -rescattering.

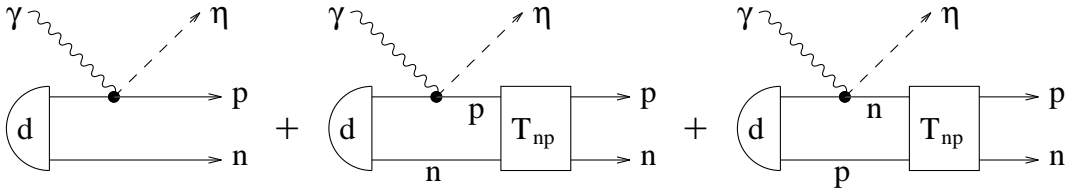


FIG. 8. Different mechanisms of the  $\gamma d \rightarrow \eta np$  process which lead to the same  $np$ -configuration in the final state.

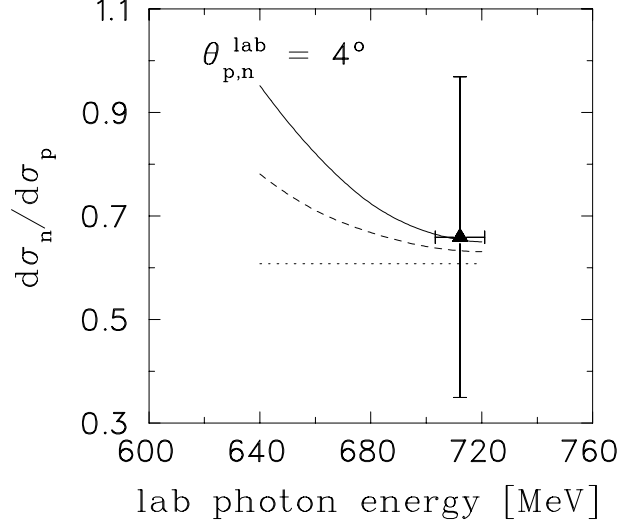


FIG. 9. Ratio of neutron to proton angular distribution calculated for the reaction  $d(\gamma, \eta N)N$  as a function of incident photon energy. The dotted curve is the free nucleon  $\sigma_n/\sigma_p$  ratio. The dashed curve shows the spectator model calculation, while  $NN$ - and  $\eta N$ -rescatterings are taken into account in the full curve. The data point is taken from the  $\eta N$  coincidence measurements of Ref. [4].

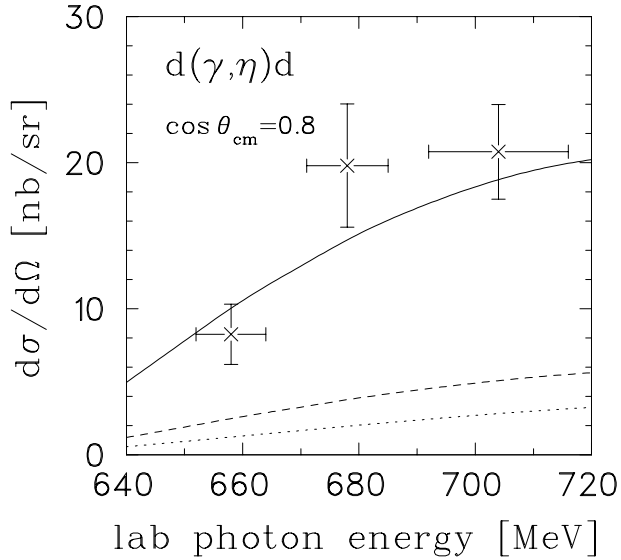


FIG. 10. Differential  $d(\gamma, \eta)d$  cross section calculated with different values of the parameter  $\alpha = t_{\gamma\eta}^{(s)}/t_{\gamma\eta}^{(p)}$ . The dotted, dashed, and full curves correspond to  $\alpha = 0.09, 0.13$  and  $0.26$ , respectively. The data are taken from Ref. [4].